

Artificial Cells: Temperature-Dependent, Reversible Li⁺-Ion Uptake/Release Equilibrium at Metal Oxide Nanocontainer Pores**

Achim Müller,* Dieter Rehder,* Erhard T. K. Haupt, Alice Merca, Hartmut Bögge, Marc Schmidtman, and Gabriele Heinze-Brückner

Dedicated to Professor Martin Jansen
on the occasion of his 60th birthday

Whereas a large number of porous materials exist as extended structures, as yet very little is known about well-defined, discrete, stable, and soluble (molecular) nanoporous capsules. These capsules allow the systematic study of processes in solution related to the uptake/release of substrates such as cations, with the possibility of extending such studies to related cation–cation countertransport processes. The prediction of the affinity of *specific* substrates for *specific* areas of the capsule is of particular interest as insight may be gained into a new type of chemistry that could be performed under confined conditions.

This is the case for spherical nanosized capsules based on the rather robust fundamental skeleton (pent)₁₂(linker)₃₀ ≡ {(Mo^{VI})Mo₅^{VI}O₂₁(H₂O)₆}₁₂{Mo₂^VO₄(ligand)}₃₀, such as in **1**,^[1] which is often employed as the starting material for other related compounds as it is easily prepared.^[2] The capsules have sizeable pores and finely sculptured interiors inbetween which lie functionalized channels that display unprecedented molecular-scale filter properties.^[3a] The size and charge of the capsules can be varied (Figure 1), whereas their affinity for (special) cations depends not only on the charge but also on the nature of the functional groups present inside the cavities.^[3b] This allows the transfer of ions in a controlled and specific fashion, reminiscent of the processes that already occur in Nature on a cellular level. With respect to cation-uptake processes and the competitive uptake/release of different cations (countertransport processes), the capsules

[*] Prof. Dr. A. Müller, A. Merca, Dr. H. Bögge, M. Schmidtman, G. Heinze-Brückner
Lehrstuhl für Anorganische Chemie I
Fakultät für Chemie der Universität
Postfach 100131, 33501 Bielefeld (Germany)
Fax: (+49) 521-106-6003
E-mail: a.mueller@uni-bielefeld.de

Prof. Dr. D. Rehder, Dr. E. T. K. Haupt
Institut für Anorganische und Angewandte Chemie
der Universität Hamburg
Martin-Luther-King-Platz 6, 20146 Hamburg (Germany)
Fax: (+49) 40-42838-2893
E-mail: dieter.rehder@chemie.uni-hamburg.de

[**] The authors gratefully acknowledge the financial support of the Deutsche Forschungsgemeinschaft, the Fonds der Chemischen Industrie, the Volkswagenstiftung, and the European Union (HPRN-CT-1999-00012). A. Merca thanks the "Graduiertenkolleg Struktur-bildungsprozesse", Universität Bielefeld, for a fellowship.

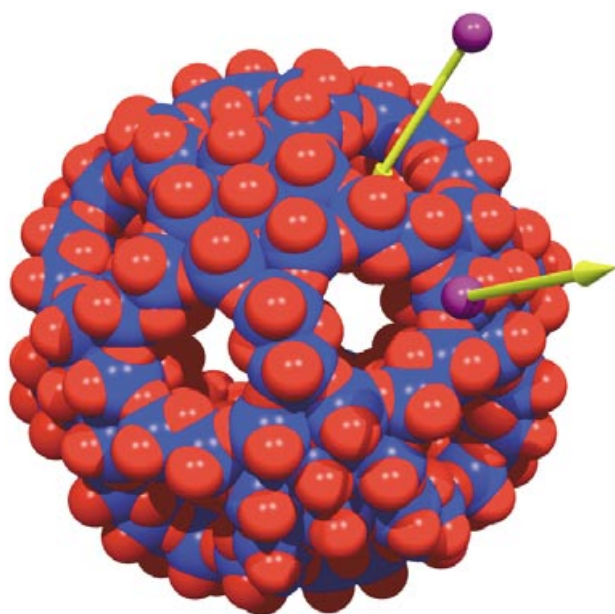
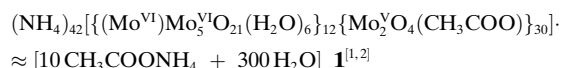


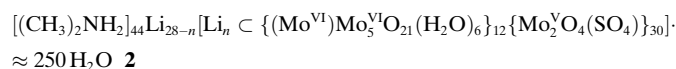
Figure 1. Schematic space-filling representation of the uptake and release of cations such as Li^+ through some of the 20 pores of highly charged anionic capsules of the structure type **2a** (Mo blue, O red).

can be considered formally as artificial cells in as much as they exhibit ion channels^[3b,c] and may allow chemistry to be performed on the nanoscale in the future.^[3d]



Herein, we report the stability and the use/applicability of this type of capsule in solution (details about the relative stabilities of capsules with different ligands in different solvents will be published later). A temperature-dependent equilibrium process that involves the uptake/release of Li^+ ions through the capsule pores and channels is also shown to be present. The results bear some relation as a model for Li^+ ion transport processes in clinical chemistry research.

The uptake/release of Li^+ ions was studied by ^7Li NMR spectroscopic analysis of solutions of compound **2**, which comprises the capsule skeleton mentioned earlier. Treatment of an aqueous solution of **1** with Li_2SO_4 in the presence of $[(\text{CH}_3)_2\text{NH}_2]^+$ cations (to render the compound soluble in DMSO) led to the formation of compound **2**, which was characterized by elemental analysis, thermogravimetry (to determine the amount of water of crystallization), flame photometry (to determine the number of Li^+ cations), redox titrations (to determine the number of Mo^{V} centers), spectroscopy (IR, Raman, UV/Vis), as well as X-ray single-crystal structure analysis^[4] (including bond valence sum calculations), and ^7Li NMR spectroscopy.^[5]



Compound **2** crystallizes in the space group $R\bar{3}$ and is soluble in H_2O and DMSO. Its anionic capsule **2a** contains

20 pores, 20 channels, and a functionalized cavity (see also reference [3a]). The incorporation of Li^+ cations can easily be detected by IR^[6a] and especially ^7Li NMR spectroscopy, but is only indirectly detected by X-ray single-crystal structure analysis. Figure 2 shows sections of the crystal structure of **2a**

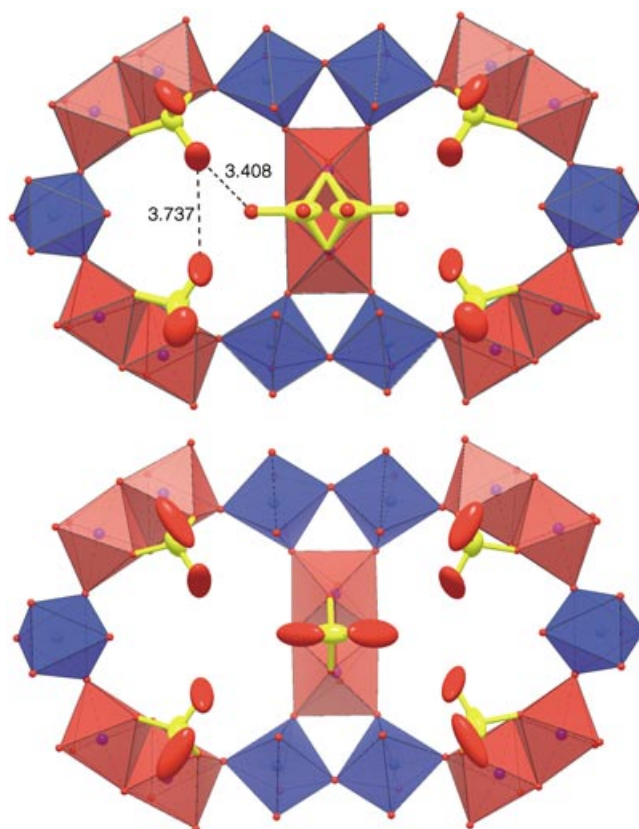


Figure 2. Outline of two of the 20 pores, as well as below-pore sections, of the anions **2a** (bottom) and the related anion **3a** (top).^[4] Whereas in the case of **2a**, the disorder could not be resolved for the SO_4^{2-} ligands—although the size and shape of their thermal ellipsoids clearly reflect the influence of Li^+ (bottom)—the disorder was successfully resolved for a sulfate ligand of **3a** (top). Shown are: 1) the Mo_6O_6 polyhedra (binuclear linkers in red) that form two adjacent pores— Mo_9O_9 rings with an average ring-aperture of $\approx 0.45 \text{ nm}$ (for example, see reference [3a]), and 2) the SO_4^{2-} ligands coordinated to the $\{\text{Mo}_2\}$ linkers below the pores. The disorder for the SO_4^{2-} ligand coordinated to the “central” $\{\text{Mo}_2\}$ group is caused by “directly non-observable” Li^+ cations, giving rise to the respective distances (top).

and of the related structure **3a**, which is abundant in the compound $\text{Li}_{65}(\text{NH}_4)_7[(\text{Mo}^{\text{VI}})\text{Mo}_5^{\text{VI}}\text{O}_{21}(\text{H}_2\text{O})_6]_{12} \cdot \{\text{Mo}_2^{\text{V}}\text{O}_4(\text{SO}_4)\}_{30} \cdot \approx 200 \text{H}_2\text{O}$ **3** $\equiv \text{Li}_{65}(\text{NH}_4)_7 \cdot \mathbf{3a} \cdot \approx 200 \text{H}_2\text{O}$; this material^[4] has a higher concentration of Li^+ ions^[5] but could not be considered in this case for NMR spectroscopic investigations as it is insoluble in DMSO.

From the present X-ray diffraction study (Figure 2), it is seen that the $\text{O} \cdots \text{O}$ distances between the three SO_4^{2-} ligands are too large ($> 3.7 \text{ \AA}$) for a symmetrical coordination of the Li^+ ion to all of the sulfate groups. Consequently, unsymmetrical coordination below the pore channels occurs (Figure 2, top). This is in contrast to the situation encountered with the larger Na^+ cations, which are symmetrically coordi-

nated to each of the three sulfate groups and which leads to a highly symmetrical $60 = 20 \times 3$ water “cluster” coordinated to the Na^+ cations.^[6b] Clearly, this is not possible in the present (unsymmetrical) case with Li^+ ions.

According to the Raman spectra, the capsules with icosahedral symmetry are quite stable in O_2 free solutions in H_2O and DMSO up to $\approx 60^\circ\text{C}$ (Figure 3). As the spectrum

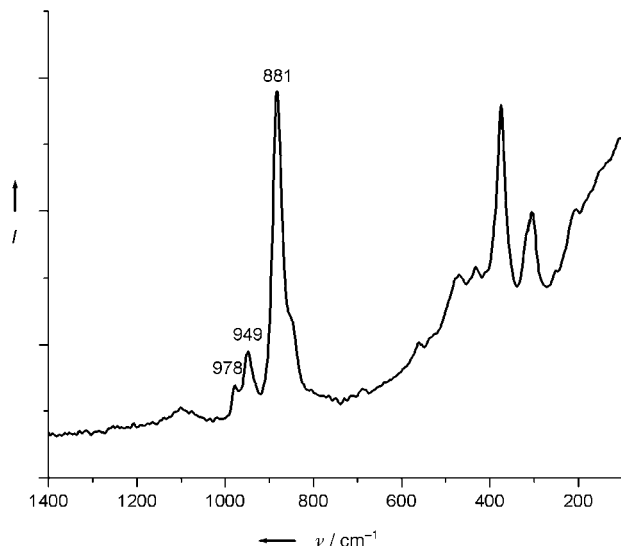


Figure 3. Raman spectrum of **2** in H_2O ($\lambda_{\text{exc}} = 1064 \text{ nm}$), which is practically identical to that of solid **2** and thus supports the reasonable stability of the highly symmetrical capsule **2a** in solution. The most intense band at 881 cm^{-1} corresponds to the totally symmetric A_g breathing vibrations of the capsule which involve predominantly $60 \mu_3\text{-O}(\text{Mo}_3)$ surface atoms.

consists of only a few lines (note the possible fivefold degeneracy expected for the I_h point group, and that only A_g and H_g type vibrations are Raman allowed) this allows the easy detection of eventual decomposition even for such an extremely large molecular system. The bands are characteristic for the highly symmetrical molybdenum oxide based $\{(\text{Mo}^{\text{VI}})\text{Mo}_5^{\text{VI}}\}_{12}[\text{Mo}_3^{\text{V}}]_{30}$ type skeleton.

The ^7Li NMR spectrum^[7] of **2** dissolved in $\text{DMSO}/[\text{D}_6]\text{DMSO}$ (1:1; $c(\text{Li}^+) \approx 50 \text{ mM}$; Figure 4) measured at room temperature shows two sharp signals at $\delta = -0.78$ and -0.80 ppm (I), which correspond to $[\text{Li}(\text{dmsO})_n]^+$ in the bulk solution (the peaks are identical to those in the spectrum of Li^+ ions in pure DMSO), and at least three broad (half-width ($W_{1/2}$) $\approx 80 \text{ Hz}$) overlapping signals centered at $\delta = -1.67$, -2.18 , and -2.56 ppm (II–IV; overall relative intensity $\approx 15\%$). These latter peaks are assigned to three different Li^+ -ion sites associated with the cluster $\text{Li}^+ \subset \mathbf{2a}$. The upfield shifts—with respect to $[\text{Li}(\text{dmsO})_n]^+$, $\delta \approx -0.79 \text{ ppm}$ —reflect the increased complexation of the Li^+ cations to negatively charged ligands such as sulfate, and/or bridging oxo groups such as at the Mo_9O_9 type rings/pores.^[8a] This pattern, which is observed immediately after the dissolution of **2**, does not change within several days; that is, the system readily reaches equilibrium and remains rather stable over an extended period of time. Furthermore, the temperature dependence of

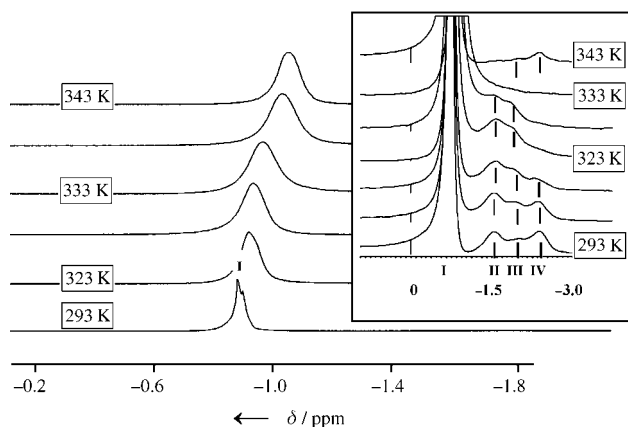
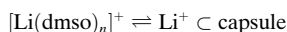


Figure 4. Variable-temperature ^7Li NMR spectra of **2** ($c(\mathbf{2}) \approx 1.8 \text{ mM}$) in $\text{DMSO}/[\text{D}_6]\text{DMSO}$ 1:1. The inset shows the vertical expansion with the uppermost spectrum obtained after cooling back to room temperature. I ($\delta = -0.79 \text{ ppm}$) corresponds to $[\text{Li}(\text{dmsO})_n]^+$, whereas II ($\delta = -1.67 \text{ ppm}$), III ($\delta = -2.18 \text{ ppm}$), and IV ($\delta = -2.56 \text{ ppm}$) correspond to Li^+ sites associated with $\text{Li}^+ \subset \mathbf{2a}$.

the spectral patterns (Figure 4) with respect to both the broadening as well as the shifts (upfield for I, downfield for II, III, and IV) of the bands upon increasing the temperature, clearly indicates an exchange equilibrium between exterior and interior Li^+ ions.^[8b] The signal at $\delta = -2.56 \text{ ppm}$ (IV) disappears at about 330 K , whereas a complete coalescence of the signals for the system (signals I, II, III, and IV) occurs at 343 K (average $\delta = -0.96 \text{ ppm}$) representing very fast exchange within the equilibrium:

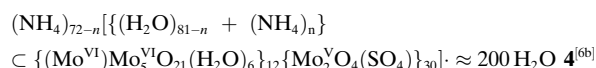


In the temperature range $293\text{--}343 \text{ K}$, the exchange process is largely reversible for two of the sites; upon cooling, the signals at $\delta = -2.18$ (III) and -2.56 ppm (IV) are almost restored. However, the signal at $\delta = -1.67 \text{ ppm}$ (II) does not reappear which suggests that one of the Li^+ -ion sites is not occupied again. The first of the upfield signals, II, is assigned to Li^+ ions coordinated to the sulfate group which was also proven from crystallographic studies and IR spectroscopic measurements. This site is the furthest distance away from the pore area/cluster periphery and is correspondingly not reoccupied after cooling as the sites closer to the capsule periphery (peaks III and IV) are the first to be reoccupied, which decreases the affinity of the capsule for cations. The more-peripheral sites have a higher electron density (in agreement with a classical Pauling rule) with the consequence that the related peaks are found at higher fields.

Complementary to the temperature-dependent behavior of the signals, the $[\text{Li}(\text{dmsO})_n]^+ \text{--} \text{Li}^+(\text{capsule})$ -exchange process has been confirmed by ^7Li - ^2D exchange spectroscopy (EXSY) of solutions of **2** in DMSO ($c(\mathbf{2}) = 1 \text{ mM}$; $c(\text{Li}^+) = 30 \text{ mM}$; slow exchange conditions at room temperature and a mixing time of 1.5 s were employed). The EXSY spectrum (not shown here) displays cross-peaks owing to a magnetization transfer between external (signal I) and internal Li^+ ions (signals II–IV) which disappear upon the addition of an

excess of guanidinium chloride ($c = 30$ mM); guanidinium cations prevent exchange through blockage of the capsule pores (see reference [6c]). Concomitantly, signals II and III almost disappear and a new signal representing 5% of the overall integral intensity appears at $\delta = -3.1$ ppm.

Treatment of a solution of **4** in DMSO with a 20-fold molar excess of LiCl leads to the uptake/incorporation of about 12% of the Li^+ ions as observed from a broad signal at $\delta = -2.03$ ppm for $\text{Li}^+ \subset \mathbf{4a}$. This signal is accompanied by the resonance for $[\text{Li}(\text{dmsO})_n]^+$ at $\delta = -0.82$ ppm with an upfield shoulder at about $\delta = -1.05$ ppm. The situation is comparable to the system $\text{Li}^+ \subset \mathbf{2a}$ in as far as the Li^+ ions are apparently taken up by the cluster under changed conditions. In the case of the anionic capsule **4a**, for example, Li^+ competes with NH_4^+ to some extent for the capsule sites.



The present study of the uptake/release of cations by a capsule in solution may be extended to investigate nanoscale reactions in solutions (see also reference [3d]) as well as a large variety of cation-transport phenomena (e.g. competition processes) in different solvents^[9]; furthermore, unique hydration structures can be investigated under restricted conditions. An important aspect is that the interiors, sizes, and pores of the capsules can be varied to allow different cation-affinity properties. Interestingly, the transport of cations under physiological conditions (e.g. Li^+ -ion transmembrane transport and storage) can, in principle, be modeled. Also, there is the possibility to model important transport pathways of medicinal interest, such as the Li^+ - Na^+ countertransport process (of interest in hypertension research) in which Na^+ ions enter and Li^+ ions leave erythrocytes in order to maintain the Na^+ ion balance in the cells and the plasma.^[10–12]

Experimental Section

2: The pH value of a solution of **1** (2.0 g, 0.068 mmol) and $\text{Li}_2\text{SO}_4 \cdot \text{H}_2\text{O}$ (10 g, 78 mmol) in H_2O (80 mL) was adjusted to ≈ 2.2 with aqueous H_2SO_4 (0.5 M), and the solution was stirred for 5 h at room temperature. (The large excess of Li_2SO_4 was necessary first, owing to the large number of functional groups present in the capsule, e.g. 30 SO_4^{2-} groups and $180 \text{ Mo}_3\text{O}_9$ type O atoms, and second, to isolate the highly water soluble product **2** as a salt, and third, because of the high affinity of Li^+ to water.) The temperature of the solution was increased to 70°C over 30 min, then $(\text{CH}_3)_2\text{NH}_2\text{Cl}$ (1.5 g, 18.39 mmol) was added, and the solution was stirred at this temperature for a further 30 min. The hot solution was filtered, then the cooled dark brown filtrate was stored at 20°C to effect crystallization. After 4 days, the precipitated dark brown, parallelepiped crystals of **2** were isolated by filtration and dried in air (70% based on **1**); elemental analysis: calcd for $\text{C}_{88}\text{H}_{996}\text{Li}_{28}\text{Mo}_{132}\text{N}_{44}\text{O}_{814}\text{S}_{30}$: C 3.58, N 2.08, Li 0.65; found: C 3.6, N 2.1, Li (flame photometry) 0.6; IR (KBr): $\tilde{\nu} = 1622$ (m, $\delta(\text{H}_2\text{O})$), 1463 (w-m, $\delta_{\text{as}}(\text{CH}_3)$), 1183 (w), 1137 (m-w), 1053 (w, $\nu_{\text{as}}(\text{SO}_4)$ triplet), 975 (s), 943 (m, $\nu(\text{Mo}=\text{O})$), 860 (s), 802 (vs), 729 (s), 634 (m), 574 cm^{-1} (s); FT-Raman (see Figure 3); UV/Vis (H_2O): $\lambda = 459$ nm.

Received: January 15, 2004

Revised: May 19, 2004 [Z53762]

Keywords: artificial cells · ion channels · lithium · nanostructures · porous materials

- [1] For a review, see: A. Müller, P. Kögerler, C. Kuhlmann, *Chem. Commun.* **1999**, 1347–1358.
- [2] a) A. Müller, S. K. Das, E. Krickemeyer, C. Kuhlmann, *Inorg. Synth.* **2004**, *34*, 191–200; b) L. Cronin, E. Diemann, A. Müller in *Inorganic Experiments* (Ed.: J. D. Woollins), Wiley-VCH, Weinheim, **2003**, pp. 340–346.
- [3] a) A. Müller, S. K. Das, S. Talismanov, S. Roy, E. Beckmann, H. Bögge, M. Schmidtman, A. Merca, A. Berkle, L. Allouche, Y. Zhou, L. Zhang, *Angew. Chem.* **2003**, *115*, 5193–5198; *Angew. Chem. Int. Ed.* **2003**, *42*, 5039–5044; in all the cases studied therein, the positioning of the cations was clearly understood except for that of Rb^+ —this was attributed to the influence of the crystallization process, which does not influence the results in the present solution process. b) An extreme affinity is observed for the sulfate type capsule in the case of Ca^{2+} as 20 of these ions can be positioned at the end of the 20 channels at specific positions where also Na^+ cations, although in a smaller amount, can be positioned^[3a]—in doing so, the entrance to the central cavity is completely blocked (unpublished results). In cases where the encapsulated cation positions cannot be determined, the given charge refers to that of the empty capsule^[1,2] (see also **3**). c) Interesting cation uptake (and also the uptake of anions and water molecules) under confined conditions has also been observed for nanotube structures, but such a situation does not easily allow an equilibrium study to be performed in solution; see: T. Ohkubo, Y. Hattori, H. Kanoh, T. Konishi, T. Fujikawa, K. Kaneko, *J. Phys. Chem. B* **2003**, *107*, 13616–13622; T. Ohkubo, H. Kanoh, K. Kaneko, *Aust. J. Chem.* **2003**, *56*, 1013–1016; see also: d) “Traps for cations”: W. G. Klemperer, G. Westwood, *Nat. Mater.* **2004**, *2*, 780–781.
- [4] Crystal data for **2** ($\text{C}_{88}\text{H}_{996}\text{Li}_{28}\text{Mo}_{132}\text{N}_{44}\text{O}_{814}\text{S}_{30}$): $M = 29521.49$ g mol⁻¹, rhombohedral, space group $R\bar{3}$, $a = 32.8188(12)$, $c = 74.350(4)$ Å, $V = 69352(5)$ Å³, $Z = 3$, $\rho = 2.121$ g cm⁻³, $\mu = 1.908$ mm⁻¹, $F(000) = 43356$, crystal size = $0.30 \times 0.25 \times 0.20$ mm³; crystals of **2** were removed from the mother liquor and immediately cooled to 188(2) K on a Bruker AXS SMART diffractometer (three cycle goniometer with 1 K CCD detector, MoK_α radiation, graphite monochromator; hemisphere data collection in ω at 0.3° scan width in three runs with 606, 435, and 230 frames ($\phi = 0, 88, \text{ and } 180^\circ$) at a detector distance of 5.0 cm). A total of 135812 reflections ($1.53 < \theta < 26.99^\circ$) were collected of which 33506 reflections were unique ($R_{\text{int}} = 0.0429$). An empirical absorption correction using equivalent reflections was performed with the program SADABS. The structure was solved with the program SHELXS-97 and refined with SHELXL-97 to $R = 0.0506$ for 25064 reflections with $I > 2\sigma(I)$, $R = 0.0763$ for all reflections; max./min. residual electron density 1.613 and -1.785 e Å⁻³ (SHELXS/L, SADABS from G. M. Sheldrick, University of Göttingen 1997/2001; structure graphics with DIAMOND 2.1 from K. Brandenburg, Crystal Impact GbR, 2001). CCDC 228367 contains the supplementary crystallographic data for this paper. These data can be obtained free of charge via www.ccdc.cam.ac.uk/conts/retrieving.html (or from the Cambridge Crystallographic Data Centre, 12, Union Road, Cambridge CB2 1EZ, UK; fax: (+44) 1223-336-033; or deposit@ccdc.cam.ac.uk). Cell parameters for **3**: monoclinic space group $C2/m$, $a = 44.483(2)$, $b = 40.077(2)$, $c = 31.757(2)$ Å, $\beta = 134.116(1)^\circ$, $V = 40645(5)$ Å³.
- [5] ⁷Li NMR spectra of solutions were recorded on a Bruker Avance 400 spectrometer (155.51 MHz) in rotating 10-mm diameter tubes; acquisition time 2.1 s, relaxation delay 2 s, pulse width 30° . All data are reported relative to the reference material (9.7 M LiCl in D₂O, according to: R. K. Harris, E. D.

- Becker, S. M. Cabral de Menezes, R. Goodfellow, P. Granger, *Pure Appl. Chem.* **2001**, 73, 1795–1818). Area calibration was carried out by insertion of a coaxial inset containing LiCl (0.1 M in $[D_6]DMF$, $\delta = +0.90$). The Lorentzian line-shape analysis was performed for four lines by using the ‘deconvolution 1’ feature of the Bruker WINNMR V6.0 program.
- [6] a) Compound **2** shows a triplet 1183/1137/1053 cm^{-1} in the IR spectrum which originates from the bidentate coordination of the sulfate anion (ν_{as} mode of the “free” SO_4^{2-} ion lies at ca. 1105 cm^{-1}); see: K. Nakamoto, *Infrared and Raman Spectra of Inorganic and Coordination Compounds*, 5th ed., Wiley, New York, **1997**, Part A, p. 199; Part B, pp. 79–82. As the SO_4^{2-} groups are located *trans* to the Mo=O bonds the coordination is rather weak, with the consequence that the “terminal” sulfate O atoms show a higher electron density than in the case of a stronger ligand coordination. This can strengthen (relatively) the interaction with encapsulated cations, being again stronger for Li^+ ions than in general for Na^+/NH_4^+ ions (note that one Na^+ ion is coordinated to three sulfate ligands in the capsule, whereas Li^+ is predominantly coordinated to one SO_4^{2-} group and so the interaction per sulfate ligand is therefore larger).^[6b] In the case of related Na^+/NH_4^+ salts, the two bands at higher energy are observed at nearly the same wavenumbers as the corresponding bands for **2a**, whereas the lower energy band of the triplet occurs at $\approx 1040\text{ cm}^{-1}$ in the Na^+/NH_4^+ salts but at 1053 cm^{-1} in the case of **2a**. The same situation as in the case of the Na^+ and NH_4^+ capsules is found for a compound containing only guanidinium cations, which cannot enter the cavity;^[6c] this band consequently is also observed at 1038 cm^{-1} . (The assignment of the respective band for the guanidinium compound was rather difficult as it partially overlaps with the $O_2PH_2^-$ -bands).^[6c] The shift of the band in the case of **2a** is influenced by the rather strong interaction with Li^+ ions which partially decreases the negative charge on the sulfate and therefore strengthens the S–O bonds; b) A. Müller, E. Krickemeyer, H. Bögge, M. Schmidtman, B. Botar, M. O. Talismanova, *Angew. Chem.* **2003**, 115, 2131–2136; *Angew. Chem. Int. Ed.* **2003**, 42, 2085–2090; the compound **4** can be obtained more easily and methodically (without the need for heating) by acidification of the solution to protonate the acetate ligands and render them better leaving groups; c) A. Müller, E. Krickemeyer, H. Bögge, M. Schmidtman, S. Roy, A. Berkle, *Angew. Chem.* **2002**, 114, 3756–3761; *Angew. Chem. Int. Ed.* **2002**, 41, 3604–3609.
- [7] a) J. W. Akitt in *Multinuclear NMR* (Ed.: J. Mason), Plenum, New York, **1987**, chap. 7; b) C. Detellier in *NMR of Newly Accessible Nuclei*, Vol. 2 (Ed.: P. Laszlo), Academic Press, New York, **1983**, chap. 5; c) B. Lindmann, S. Forsén in *NMR and the Periodic Table* (Eds.: R. K. Harris, B. E. Mann), Academic Press, New York, **1978**, chap. 6.
- [8] a) The notation “increased complexation of Li^+ ” refers to the dominance of the paramagnetic contribution related to variations in shielding. In other words, paramagnetic shielding is expected to decrease (and overall shielding to increase) with the increasing expansion of the “electron cloud” around Li, to result in an increased covalency of the Li^+ –donor interaction as the contact between the Li^+ ion and the donor groups becomes more intimate. The signal IV could be attributed to the complexation of Li^+ ions by the oxo functions of the Mo_9O_9 ring, as this peak disappears the most easily, both upon heating and upon the addition of Na^+ ions. For the crown ether complex $[Li(15C5)]^+$, which may be compared to the coordination of Li^+ ions in the present study, a chemical shift value of $\delta = -1.8$ ppm was noted; see: A. I. Popov, *Pure Appl. Chem.* **1979**, 51, 101. Importantly, the Mo^V centers in the binuclear unit are spin-coupled upon formation of a metal–metal bond, thereby excluding influences by paramagnetic centers; b) for an *independent resonance signal*, deshielding is expected upon an increase in the temperature as a consequence of the increased paramagnetic-deshielding contributions as the vibronic levels of the ground and excited states become more populated. Concomitantly, if the nucleus is quadrupolar as in the case of 7Li , the resonance should sharpen upon a decrease in the molecular correlation time (decreasing viscosity). In the present case, an increase in the shielding and broadening of the line widths is observed for signal I as the temperature is raised; the spectral patterns clearly indicate an exchange between exterior (I) and interior Li^+ ions (II, III, and IV).
- [9] For **2** dissolved in H_2O/D_2O , only one narrow 7Li resonance at $\delta = -0.16$ ppm ($W_{1/2} = 2.3$ Hz) is observed, which corresponds to hydrated Li^+ ions and is indicative of the complete extrusion of Li^+ ions into the aqueous medium. This arises from the higher affinity of Li^+ for water than for the functional capsule sites. Competitive-phenomena studies (e.g. Li^+/Na^+) performed in aqueous media in the presence of electrolytes (to reduce the affinity of the cations for the solvent, and to approximate physiological conditions) are currently underway. As far as the dielectric properties of the medium are concerned, serum and cytosol more closely resemble DMSO than water. Note that more than ten billion proteins are abundant in an animal cell and influence the properties of the water solvent.
- [10] Na^+ – Li^+ countertransport is an ion-transport process that exchanges sodium ions for lithium ions or other univalent cations. It was brought to clinical attention by Canessa et al., who reported that its activity was enhanced in the erythrocytes of patients with essential hypertension—a finding that was confirmed in many epidemiological and clinical studies thereafter; see: M. Canessa, N. Adragna, H. S. Solomon, T. M. Conolly, D. C. Tosteson, *New Engl. J. Med.* **1980**, 302, 772–776; P. Strazzullo, A. Siani, F. P. Cappuccio, M. Trevisan, E. Ragone, L. Russo, R. Iacone, E. Farinero, *Hypertension* **1998**, 31, 1284–1289. Although the capsule wall of our structure cannot be compared with the red-cell membrane, which perfectly balances the concentrations of cations and water so that the cells do not shrink, nevertheless, it allows fundamental countertransport phenomena to be measured; see: Y. Yawata, *Cell Membrane: The Red Blood Cell as a Model*, Wiley-VCH, Weinheim, **2003**.
- [11] Numerous papers are being published on the influence of Li^+ ions on many biochemical and pathobiochemical processes owing to its high positive-charge density, but a complete picture of the medicinal and biochemical properties of Li^+ is not yet available. In any case, Li^+ ions play a key role in the treatment of bipolar disorder (manic depression), the mechanism of which is not known; for examples, see: H. R. Pilcher, *Nature* **2003**, 425, 118; S. J. Lippard, J. M. Berg, *Bioinorganische Chemie*, Spektrum, Heidelberg, **1995**; *Principles of Bioinorganic Chemistry*, University Science Books, Mill Valley, USA, **1994**. It has been reported that Li^+ ions block the recycling pathway for inositol-1,4,5-triphosphate (IP_3); malfunctions of the inositol system have been linked to a number of illnesses, including manic depression and cancer; see: G. Thomas, *Medicinal Chemistry: An Introduction*, Wiley, Chichester, **2000**.
- [12] Preliminary experiments directed towards competition in the uptake/release of Li^+ and Na^+ ions show that for $c(Li^+) = 30$ mM and $c(Na^+) = 15$ mM (in the form of NaBr), almost all of the “capsule-bound” Li^+ ions are replaced by Na^+ ions; that is, about 98 % of the Li^+ ions are present in the form of $[Li(dmsO)_n]^+$ (signal I), whereas about 70 % of the Na^+ are bound to the capsule ($\delta(^{23}Na) = -1.5$ and -12 ppm ($W_{1/2} = 2.6$ kHz) for $[Na(dmsO)_n]^+$ and $Na^+C\mathbf{2a}$, respectively). This is a remarkable result that shows the relatively high affinity of the capsule for Na^+ as they block/close the pores/channels^[6b] (different aspect in ref. [6]).